Quantum coherence in the photosynthesis apparatus of living cyanobacteria

Tim Rammler[1,2], Frank Wackenhut[1], Sven zur Oven-Krockhaus[1,2], Johanna Rapp[3], Karl Forchhammer[3], Klaus Harter[2], Alfred J. Meixner[1]

[1]Institute of Physical and Theoretical Chemistry, University of Tübingen, Tübingen, Germany
[2]Center for Plant Molecular Biology, University of Tübingen, Tübingen, Germany
[3]Interfaculty Institute of Microbiology and Infection Medicine, University of Tübingen, Tübingen, Germany

Abstract

Life as we know it cannot exist without photosynthesis, and even though the main photosynthetic mechanisms have been well investigated, some aspects are still unresolved. One example is the energy transfer to the reaction centers by accessory photosynthetic pigments after the absorption of photons. This process has an extremely high efficiency, which cannot be explained by a classical Foerster resonance energy transfer. However, a quantum mechanical process based on a coherent or wave-like energy transfer may provide an explanation for the high efficiency. In order to determine whether nature makes use of such a coherent process, we influence the potential coherence of photosynthetic pigments *in vivo* using an optical microresonator, which consists of two parallel silver mirrors separated only by the distance of a few wavelengths. The electromagnetic field inside such a microcavity is strongly confined, enabling coherent light-matter coupling. Here, we embedded living cyanobacteria of the species *Synechococcus elongatus* (strain PCC 7492) into the microresonator and exposed them to the confined electromagnetic field. The observation of vacuum Rabi splitting and anti-crossing observed in the transmission- and fluorescence spectra provides evidence of coherent coupling of the pigments with the resonator modes without harming the bacteria. Furthermore, we showed that not only some photosynthesis pigments are involved in this coupling, but all pigments in the excitation focus are coupled coherently. Our findings shed light on the function of quantum coherence in the evolution of photosynthetic organisms.

Introduction

The idea that quantum mechanical phenomena may play a significant role in biology has fascinated researchers for a long time. Erwin Schroedinger suspected, as early as 1944, that quantum mechanics have a direct influence on biology and evolution.[1] Conversely, Alexander Sergejewitsch Davydov stated about 40 years later (1982) that quantum mechanical processes are only relevant for purely isolated systems and therefore of little relevance to biological systems.[2] He assumed that fragile quantum phenomena were probably not important for the "warm, wet and loud" creatures.[3] However, this opinion changed dramatically in 2010, when for the first time quantum biological phenomena, such as quantum coherence, were measured in isolated photosynthetic complexes at physiologically relevant temperatures.[4] Besides the prime example of photosynthesis, other biological phenomena are also currently suspected of being driven by quantum mechanics. In proteins and enzymes, it is assumed that quantum mechanical effects, such as long-range electron transfer[5] and proton tunneling[6], are involved. Also under discussion is the magnetoreception[7] of some animals for geomagnetic orientation.

In photosynthesis, light energy is absorbed and converted into relatively stable chemical products by membrane-integral pigment-protein complexes called photosystems. Photosynthetic complexes are optimized to capture solar light and to transmit the excitation energy from the peripheral pigments to the photosynthetic reaction centers where the processes for long-term energy storage begin.

The efficiency of this energy transfer is extremely high (close to $100\,\%$[3]). Its mechanism is often described by classical models that involve “hopping”[8] of excited-state populations along discrete energy levels (Fig. 1A). These energy levels and their coupling to the reaction centers were mapped and measured in isolated photosynthetic complexes from *Chlorobium tepidum* by 2D-Fourier transform electronic spectroscopy.[9] However, these models do not fully explain the unusually high efficiency of energy transfer, requiring us to look beyond the classical approach to quantum mechanics. Wavelike energy transfer arising from the quantum coherence in the photosynthetic complexes was first predicted and then measured at $77\,K$ and later at ambient temperature, again in isolated photosynthetic complexes from *Chlorobium*[4], offering a possible explanation for the fast and almost lossless energy transfer from the peripheral pigments to the reaction centers (Fig. 1B). In addition, there are several other studies on the topic of coherence in the photosystem of bacteria *in vivo* and under physiological conditions. [9] [10] [11] [12] [13] [14] [15] [16] [17]

However, photosynthesis-related quantum mechanical processes and their physiological relevance have not yet been studied in living photosynthetic organisms. It is, therefore, not clear whether the occurrence of quantum phenomena, such as coherence, is an evolutionary byproduct or whether coherence might even be a pre-requisite for the function of the photosynthetic machinery, and thereby provide an active selection advantage in the development of photosynthetic organisms

To address this open question, we chose the cyanobacterium *Synechococcus elongatus* (strain PCC 7942) to determine quantum mechanical effects *in vivo*. Comparably to the chloroplasts of higher plants, *S. elongatus* performs oxygenic photosynthesis using water as the electron donor. The photosynthetic light reactions of cyanobacteria, such as *S. elongatus*, are essentially carried out by two trans-membrane protein complexes located in the thylakoid membrane: photosystem II (PS2) and photosystem I (PS1)[18] connected by the cytochrome b_6f complex. Together with the cytochrome b_6f complex, these molecular machines perform the light-driven electron transport to provide reduction

equivalents and generate an electrochemical proton gradient across the thylakoid membrane for the synthesis of ATP[18]. Light harvesting within the photosystems for the use of the captured energy in photosynthetic reaction centers is achieved by protein-anchored chlorophyll molecules[18]. In cyanobacteria, this intrinsic light-harvesting machinery is supported by peripheral pigment complexes - the phycobilisomes (PBS) - anchored to the photosynthetic reaction centers. With 3 to 7 MDa, PBS supercomplexes are comparably huge[19], contain three different pigments and account for up to 60 % of the cyanobacterial soluble protein content[20]. The structure and spatial organization of the PBS and intrinsic antennae enables an energy transfer to the photosynthetic reaction centers within femtoseconds after light absorption[21] [22].[23] Owing to the extensive data available on *S. elongatus* regarding structure, spatial organization, dynamics and function of the photosynthetic processes, it is a particularly well-suited model organism for elucidating quantum mechanical processes in living cells at relevant physiological conditions.

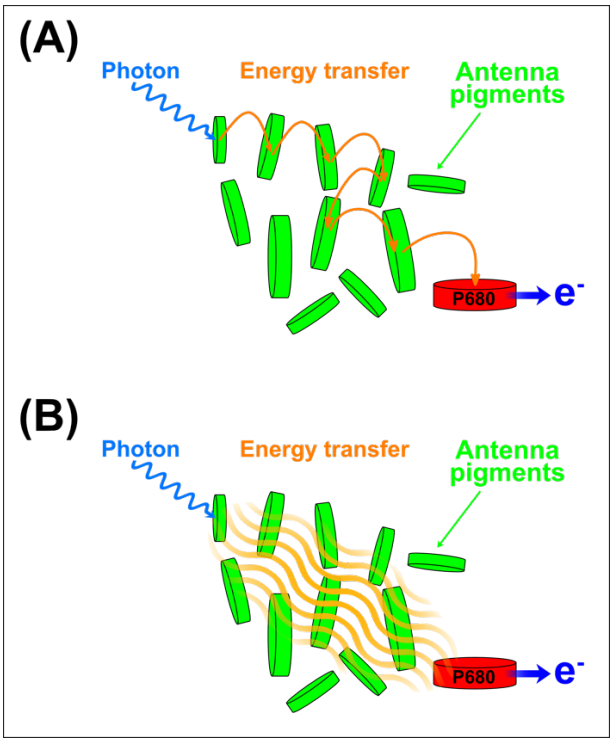

Figure 1: Models of energy transfer during photosynthesis. (A) Classical description: after the absorption of a photon (blue wavy arrow), the energy transfer from the antenna pigments (green discs) to the reaction center (i.e. P680 in light harvesting complex II (LHC II), red disc) is described by incoherent energy "hopping" (orange arrows). **(B)** Quantum mechanical description: the photon absorbed in a light harvesting complex generates a collective excitation. A superposition of the excited states results in a coherent energy transfer, possibly being the cause for the very high light harvesting efficiency (close to 100 %)[3].[24]

Methods

A Fabry-Pérot microcavity as a novel device for the *in vivo* analysis of quantum mechanical effects

To study possible quantum mechanical effects in the photosynthesis of living organisms at ambient conditions, we embedded cells of *S. elongatus* into a Fabry-Pérot optical microcavity (Fig. 2A).

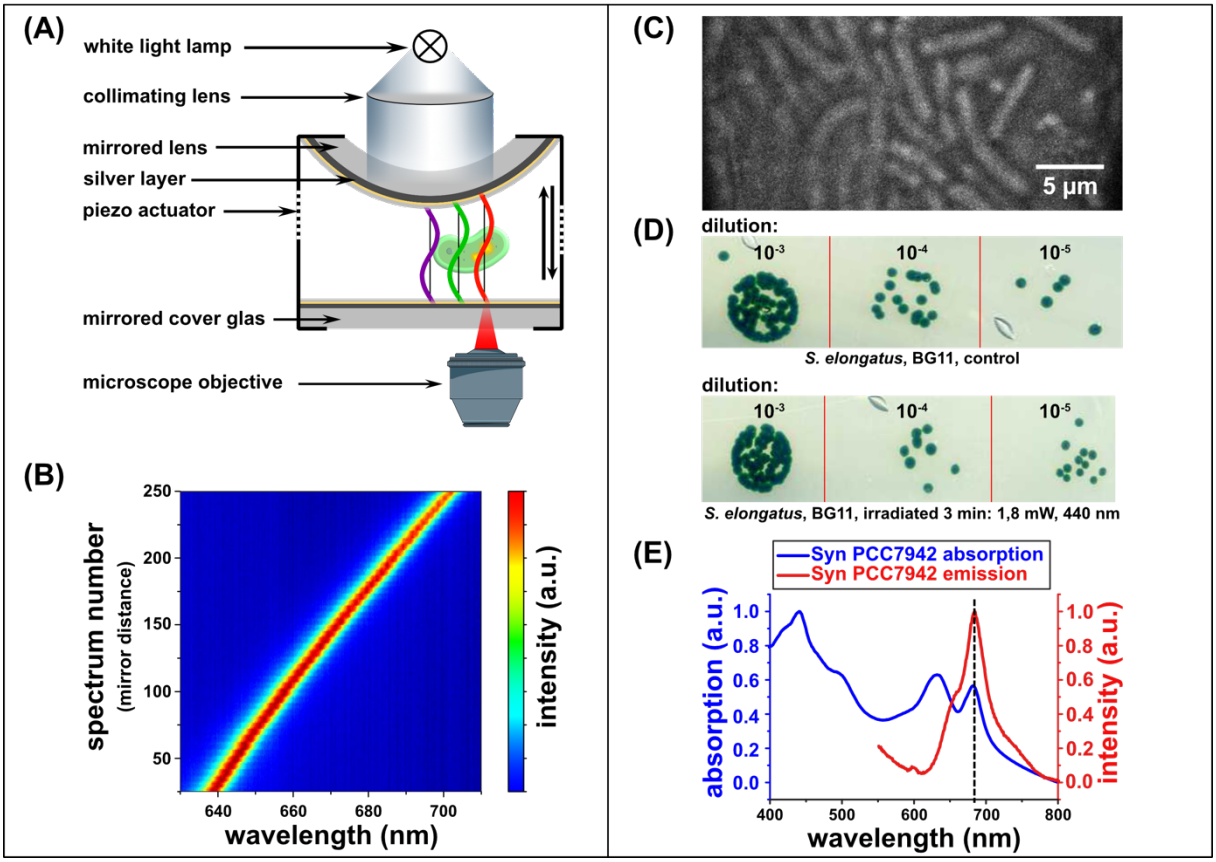

Figure 2: The spectral properties of the photosynthetic pigments of *S. elongatus* cells and a λ/2 Fabry-Pérot microcavity. The survival of *S. elongatus* cells is not impaired by the light conditions prevailing in the microcavity. (A) Scheme of the Fabry-Pérot microcavity. The microcavity consists of a semitransparent mirrored lens and a cover glass serving as a second mirror. The distance between the mirrors can be fine-tuned with piezoelectric actuators. Due to constructive and destructive interference, only wavelengths fulfilling the resonance condition of the cavity are transmitted. The bacteria are placed in an agarose matrix inside the cavity. **(B)** White light transmission spectra of the empty cavity as a function of the mirror distance. For each consecutive spectrum, the mirror spacing is increased, which shifts the resonance wavelength of the cavity accordingly. **(C)** Light microscopy image of *S. elongatus* cells inside the microcavity. **(D)** Spot assay[25] of *S. elongatus* cells in BG11 medium. Top: Non-irradiated control in a dilution series (1:10), initial concentration: $OD_{750} = 0.5$, 3-fold reproduction. Below: Irradiated sample in a dilution series (1:10), initial concentration: $OD_{750} = 0.5$, 3-fold reproduction. The bacteria were irradiated with a laser ($\lambda_{ex} = 440\ nm$, power: $1.8\ mW$) for three minutes before preparation of a drop agar assay. The growth rate is comparable to the non-irradiated bacteria, indicating a negligible impact of the typical irradiation during the experiments on the bacterial survivability. **(E)** Normalized absorption (blue) and fluorescence (red) spectra ($440\ nm$ exc.) of *S. elongatus* cells located inside the microcavity. The black dashed line indicates the wavelength where the bacteria emit and absorb photons of the same wavelength.

The microcavity consists of two semi-transparent mirrors whose distance from each other can be precisely tuned with a piezo actuator (Fig. 2A). The mirrors were produced by evaporating a $3\ nm$ thick chromium layer on a glass surface, which served as an adhesion layer for the following silver layer, which has a thickness of $30\ nm$ or $60\ nm$ for the lower and upper mirror, respectively. The thicknesses of the silver layers were optimized to give a reasonable quality factor (Q = 98) for the microcavity. Since silver is bactericidal and very susceptible to damage and oxidation, it was coated with a gold layer ($5\ nm$) and a SiO_2 layer ($20\ nm$).[26] The microcavity was assembled in a custom-built holder with piezo actuators and mounted on a confocal microscope for the collection of both white light transmission and fluorescence spectra from the same spot in the sample. Transmission spectra were acquired *via* a high numerical aperture objective lens (NA = 1.4) from below while the microcavity was illuminated by a white light source from above (Fig. 2A). The white light transmission spectra were used to determine the cavity resonance for different mirror separations as shown in Fig. 2B. Here, the mirror distance of an empty microcavity was reduced by the piezo actuators from the top to the bottom and the spectral position of the cavity resonance was tuned from $\lambda = 710\ nm$ to $640\ nm$. The upper, movable mirror was slightly curved so that the distance between the two mirrors is minimal in the center and increases radially leading to so-called Newton rings. This allows the tuning of the cavity resonance across the absorption and emission maximum of the cyanobacterial pigments *in vivo*. Fluorescence spectra and fluorescence decay curves were recorded as a function of the mirror distance by focusing a $440\ nm$ laser beam with the same high NA objective lens into the cavity.

Bacterial cultivation conditions

S. elongatus cells were cultivated under photoautotrophic conditions with continuous illumination at around $30\ \mu mol\ \text{photons}\ s^{-1}\ m^{-2}$ (Lumilux de Lux, Daylight, Osram) at $28\ °C$. The cultures were grown in $100\ mL$ Erlenmeyer flasks filled with $40\ mL$ BG11[27] medium supplemented with $5\ mM\ NaHCO_3$ and shaken at $120 - 130\ rpm$.

The survival of cyanobacteria is not impaired by the light conditions in the microcavity

The survival rate of the bacteria has to be assayed to validate the possible impact of the laser irradiation in the microcavity. Fig. 2C shows a light microscopy image of *S. elongatus* cells inside the microcavity. Due to the experimental configuration only, a single bacterium is exposed to focused laser irradiation inside the cavity and cannot be isolated after the experiment. Therefore, we designed an assay to analyze comparable irradiation intensities in bulk by embedding a bacterial culture in a low-melting agarose matrix outside the cavity. The bacteria were then exposed to high light intensities ($440\ nm$, $1.8\ mW$, $3\ min$), while a non-irradiated culture served as a control. The survivability was analyzed by a spot assay: The *S. elongatus* cultures of both treatments were adjusted to an optical density (OD) of 0.5 and a dilution series to the power of 10 was made in BG11 medium ($10^0 - 10^{-5}$). $5\ \mu L$ of each dilution was dropped on BG11-agar plates and cultivated at $28\ °C$[28] under constant light with the intensity of $30\ \mu mol\ \text{photons}\ \text{s}^{-1}\ \text{m}^{-2}$ for 7 days. As shown in Fig. 2D, no obvious growth difference between the irradiated and non-irradiated sample was observed, indicating that light conditions in the microcavity have no discernible impact on the survivability of the cyanobacteria.

Results

The spectral properties of *S. elongatus´* photosynthetic machinery can be captured in the microcavity

To characterize the spectral properties of the photosynthetic pigments, absorption and emission spectra were recorded from $20\ \mu L$ of cyanobacterial suspension, embedded in a low-melting agarose matrix to prevent cell movement (Fig. 2E). The absorption spectrum features four distinct bands: the soret band of chlorophyll at $440\ nm$[29], the carotenoid band at $500\ nm$[30], the PBS band at $630\ nm$[31] and the Q_y band of chlorophyll at $680\ nm$[32]. Excitation of the soret band proved to be very efficient, taking additional advantage of the large Stokes shift separating the laser reflection at the cavity mirrors from the emission signal, which was dominated by the chlorophyll emission at $680\ nm$.[30] Importantly, the absorption and emission spectra showed significant overlap (Fig. 2E), demonstrating that the bacteria are able to reabsorb their own emitted light. This unique photophysical feature of *S. elongatus* drastically increases the chance that its photosynthetic pigments can strongly couple to an optical field confined by a microcavity.

The microcavity influences the photosynthetic processes in living cyanobacteria

To determine whether the influence of the microcavity on the cyanobacterial photosynthetic system is detectable *in vivo*, fluorescence lifetimes (FLT) of the photosynthetic pigments by time correlated single photon counting (TCSPC) were acquired.[33]

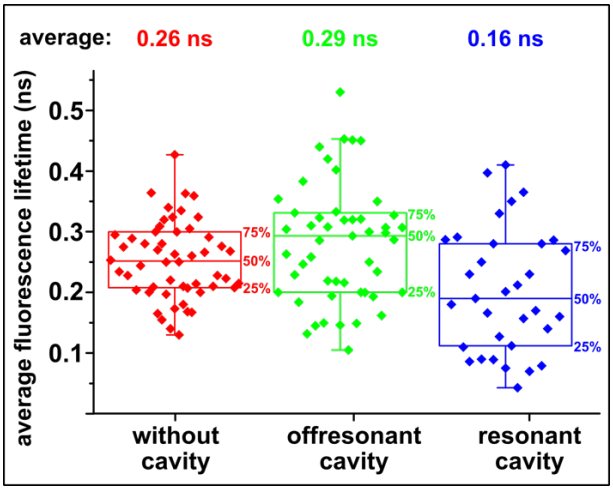

Figure 3: The average intensity-weighted FLT of the *S. elongatus* photosynthetic pigments is influenced *in vivo* by the microcavity. The bacterial cells were embedded in low-melting agarose and irradiated with ultrashort laser pulses ($\lambda_{ex} = 440\ nm$) with a duration of less than $80\ ps$ with a repetition rate of $80\ MHz$. The average intensity-weighted FLTs after pigment excitation were recorded either outside of the cavity (red), inside the off-resonance cavity (green) or inside the cavity in resonance with the light emission of the cyanobacteria (blue). An analysis of variances (ANOVA) confirms a significant difference between the fluorescence lifetimes for the off-resonant cavity and the resonant cavity.

The pigments of the photosynthetic light-harvesting complexes serve to rapidly transfer light energy to the reaction centers and, therefore, show very short individual FLTs in the sub-nano-second range.[34] The FLT properties of the pigments embedded in the light harvesting complexes of the bacteria are

more complex than those of a unimolecular dye, since every cell contains a different amount of pigments in a highly complex structural arrangement. However, these complex FLT properties can be described as a sum of exponential functions, from which an accurate average intensity-weighted FLT can be deduced (see Supporting Information for details). Therefore, the average intensity-weighted FLT can be regarded as an intrinsic property of the entire bacterial photosynthetic apparatus[35] in free space (outside the microcavity). However, the FLT can be modified by the microcavity due to a change in the spontaneous emission rate, which is known as the Purcell effect[36]. Therefore, the FLT of photosynthetic pigments *in vivo* was analyzed for three cases: (i) free space, (ii) inside the cavity in off-resonance mode and (iii) inside the cavity in resonance mode. Short laser pulses ($\lambda_{ex} = 440\,nm$) of less than $80\,ps$ and with a pulse rate of $80\,MHz$ were used. The measurement of the FLT of the pigments irradiated in free space (i) revealed a value of $\tau_I = (0.26 \pm 0.006)\,ns$ (Fig. 3). The FLT of the cyanobacterial pigments in the off-resonant microcavity (ii) was $\tau_I = (0.29 \pm 0.016)\,ns$ and did not significantly differ from the values recorded outside the cavity (Fig. 3). In contrast, the FLT in the resonant microcavity (ii) decreased to $\tau_I = (0.16 \pm 0.006)\,ns$ and was significantly shorter compared to the data recorded in free space or in the off-resonant cavity. This result is consistent with the Purcell effect and demonstrates that there is a detectable interaction between the microcavity and the photosynthetic processes in living cyanobacteria.

Strong coupling between the microcavity and the bacterial photosynthetic pigments exists *in vivo*

To study the quantum optical interaction, i.e. strong coupling, between the optical field in the microcavity and the photosynthetic machinery *in vivo*, we investigated the dispersive behavior of the coupled system. In general, the coupling of a quantum system with the optical field in a microcavity can be separated into two regimes: the strong and the weak coupling regimes. In the weak coupling regime, the respective damping constants of the cavity mode and the photosynthetic pigments are larger than the respective coupling constant. In this case, the microcavity only influences the spontaneous emission rate by the Purcell effect that was observed in the FLT analysis (Fig. 3). However, if the coupling constant exceeds the individual damping constants, a coherent energy exchange between the cavity and the photosynthetic pigments does occur and leads to so-called strong coupling.[37] The energy is then coherently transferred back and forth between the cavity mode and the photosynthetic pigments in the bacteria, which, in theory, should result in new cavity-bacteria hybrid modes. These modes are a coherent superposition of the cavity mode and the electronic state of the photosystems (polaritonic modes) as schematically illustrated in Fig. 4A/B.

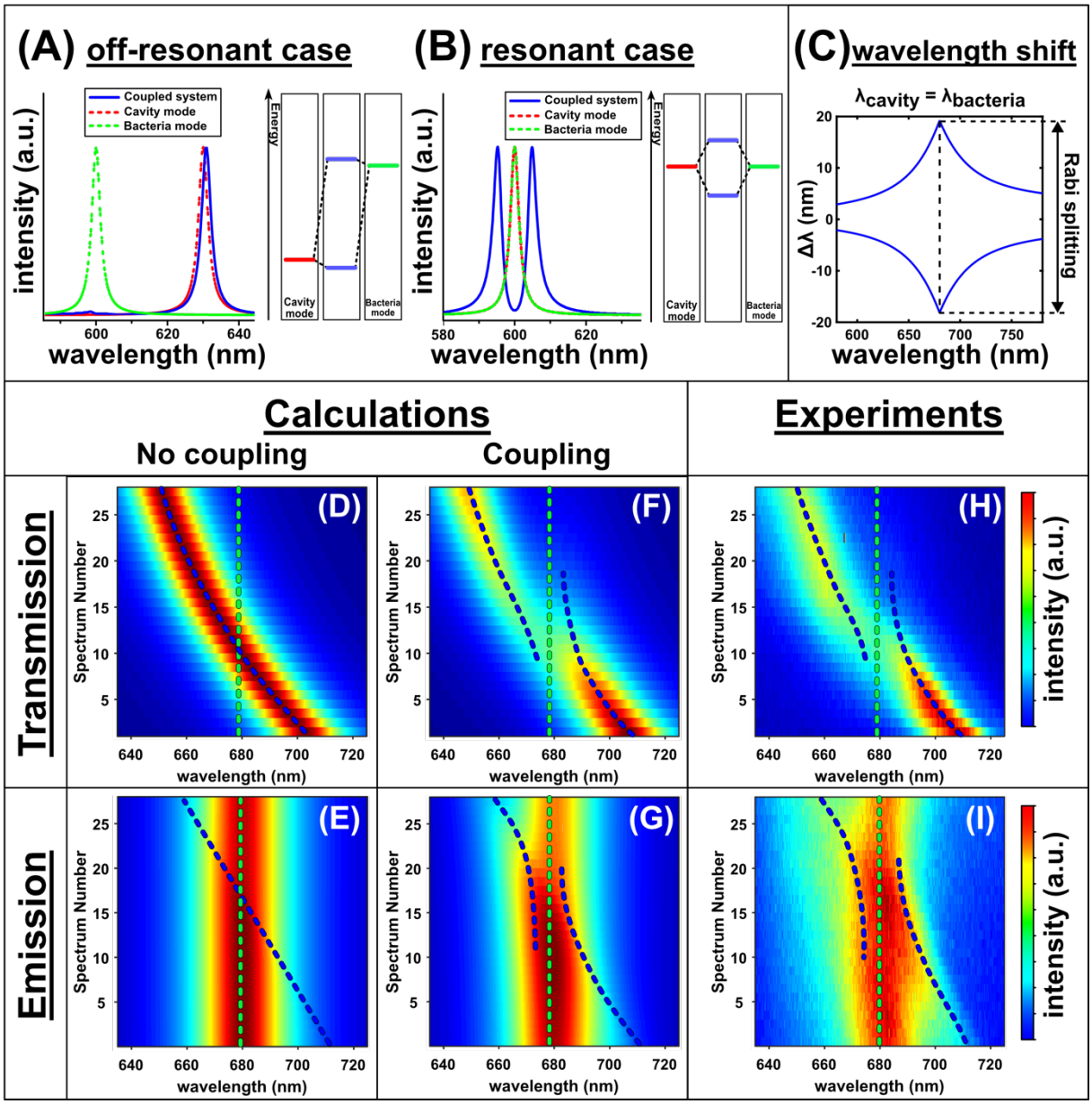

Figure 4: Strong coupling between a microcavity and the photosynthetic machinery of living cyanobacteria. **(A)** The dashed green and red spectra represent the uncoupled bacteria emission/cavity mode. The blue spectrum illustrates the cavity transmission spectrum for the non-resonant but coupled case and is similar to the uncoupled system. The graph on the right illustrates the corresponding energy level scheme. **(B)** Illustration of the resonant case, where the cavity mode is spectrally overlapping with the bacteria emission and two polaritonic modes (blue lines) are clearly visible in the cavity transmission spectrum. The energy level scheme on the right shows that the energy difference between the uncoupled states and the polaritonic modes is strongest for this case. **(C)** Wavelength shift $\Delta\lambda$ of the coupled modes relative to the uncoupled ones. The largest splitting, i.e. the Rabi splitting, is observed when the cavity and bacteria are in resonance. **(D)** Simulated cavity transmission spectra without coupling as a function of the mirror distance (indicated by the spectrum number). The green dashed line is the spectral position of the uncoupled emission of the bacteria. **(E)** Simulated bacteria emission spectra as a function of the mirror distance without coupling between the cavity mode and the bacteria. The red dashed line represents the uncoupled cavity mode. No anti-crossing can be observed in D and E when the cavity mode is tuned across the bacteria emission. **(F)** Simulated cavity transmission spectra including strong coupling between the cavity mode and the bacteria emission. **(G)** Simulated emission spectra including strong coupling. Strong coupling is visible in F/G by the anti-crossing dispersion, when the cavity mode is close to the emission of the bacteria. **(H)** Experimental

transmission spectrum of the microcavity containing cyanobacteria. **(I)** Experimental bacteria emission spectrum inside the cavity. Strong coupling can be observed in H/I by the anti-crossing dispersion and is in excellent agreement with the simulation in F/G.

The green (photosystem emission) and red (cavity mode) dashed lines in Fig. 4A/B illustrate the uncoupled bacteria emission and the cavity mode, respectively. Fig. 4A illustrates the case when there is no spectral overlap between the cavity mode and the emission of the bacteria. The transmission spectrum of such a coupled, but off-resonant, system is shown in blue and is similar to the uncoupled cavity mode. Conversely, when the cavity mode approaches the spectral position of the bacteria emission, a splitting into two polaritonic modes can be observed (Fig. 4B, blue line). Fig. 4C presents the wavelength shift $\Delta\lambda$ of the coupled modes relative to the uncoupled modes. The shift $\Delta\lambda$ caused by strong coupling is largest when the cavity is in resonance with the bacteria emission. In this case, the spectral distance between the two polaritonic modes is called Rabi splitting. Mathematically, such a coupled system can be modeled by two coupled damped harmonic oscillators, which is described in the supporting information or in [38]. First, the case is illustrated without coupling ($\kappa = 0\ eV$) between the cavity mode and the bacteria and the results were shown in Fig. 4D/E. Each line in Fig. 4D shows a calculated cavity transmission spectrum, which is indicated by spectrum number, and its intensity is given by the color map. In this simulation, the cavity length is gradually increased from the top to the bottom, which leads to a spectral redshift of the cavity resonance. The dashed lines in Fig. 4D/E represent the spectral position of the uncoupled bacteria emission and the cavity mode, respectively. Due to the absence of coupling, no splitting can be observed even when both modes have the same eigenfrequency and the bacteria emission in Fig. 4E is only influenced by the Purcell effect. However, this changes, when there is strong coupling between the cavity mode and the bacteria, which is calculated with a coupling constant $\kappa = 0.14\ eV$ in Fig. 4F/G. The calculated cavity transmission spectra in Fig. 4F show (a) clear anti-crossing behavior when the cavity resonance approaches the spectral position of the bacteria emission at $680\ nm$. However, the mode splitting is less obvious in the calculated bacteria emission spectra in Fig. 4G because it is obscured by the spectrally broad fluorescence of the bacteria.

By comparing the simulations in Fig. 4D/E with Fig. 4F/G, it was clearly possible to experimentally distinguish between no/weak and strong coupling in the microcavity-bacteria system. Excitingly, the experimental transmission and emission spectra from the living cyanobacteria showed a clear anti-crossing behavior in the cavity transmission spectra (Fig. 4H) and to a lesser extent in the emission spectra (Fig. 4I). The experimental data is in perfect agreement with the calculated spectra of Fig. 4F/G, respectively, and proves that strong coupling between the microcavity and the cyanobacteria can be achieved *in vivo*.

The coherent energy transfer involves all pigments of the cyanobacterial photosynthetic machinery

The above result shows that there is a coherent energy exchange between the cavity mode and at least some pigments of the cyanobacteria. As already shown in [39] that the photosynthesis apparatus must be described as a quantum system and that there must be an entanglement of the pigments. However,

an important question is whether interaction with the cavity induces a coherence between all photosynthetic pigments. According to the Jaynes-Cummings model, the splitting energy ΔE_n can be calculated as follows[37]:

$$\Delta E = 2\sqrt{n}\hbar g_o \qquad (1)$$

where g_0 is the vacuum Rabi splitting and n the number of fluorophores participating in the coupling. According to equation (1), the energy splitting is proportional to the square root of the number of fluorophores that coherently couple to the cavity mode. Therefore, the splitting energy should reduce when the number of fluorophores is diminished.

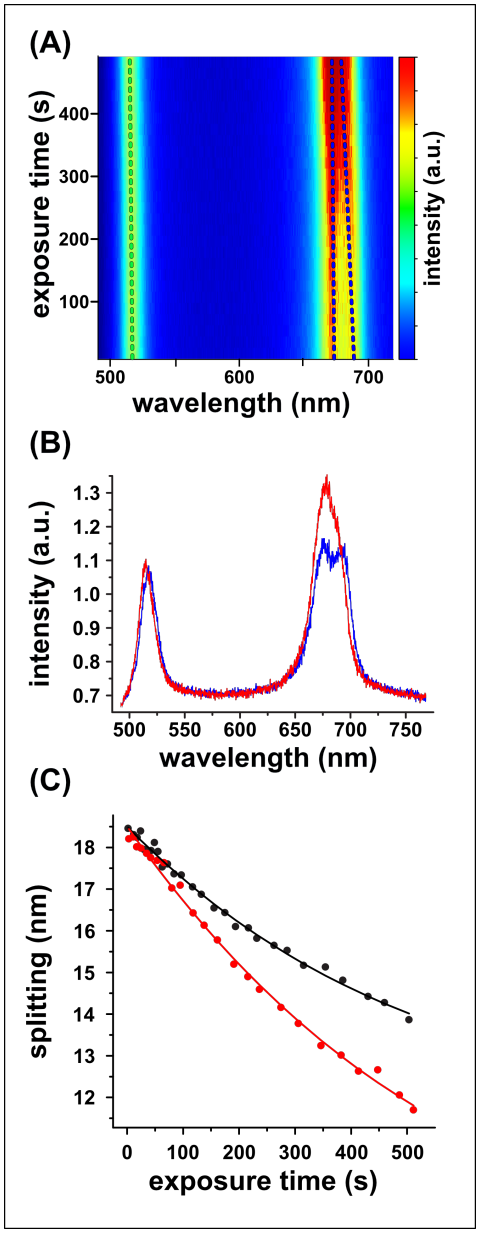

Figure 5: By photo-bleaching fluorophores and thus reducing the number of fluorophores participation in the coupling it is shown that all pigments in the focus are coherently coupled. (A) Cavity transmission spectra with two cavity resonances as a function of the exposure time. Two resonances are visible, one strongly coupled (blue dashed line) and one not coupled (green dashed line). The splitting energy und hence the coupling becomes smaller due to the continuous illumination (photo-bleaching) of the bacteria. **(B)** First (blue line, $t = 0\ ms$) and last (red line, $t = 500\ ms$) spectrum of (A). **(C)** Splitting between the two coupling peaks at $680\ nm$ as a function of the

exposure time. The two series are obtained from different spatial locations in the cavity and show the same trend with increasing bleaching of the fluorophores. The solid lines show an exponential decay fitted to the experimental data.

To experimentally reduce the number of functional pigments, the laser intensity was enhanced by the factor of 100 compared to the previous experiments, leading to photobleaching of the pigments. Two cavity resonances were observed (Fig. 5A): The first resonance at $\lambda = 546\,nm$ did not strongly couple to the cyanobacteria and therefore no change in intensity or spectral position was observed, which proves that no spatial drift occurred during the experiment. However, the second mode at $\lambda = 680\,nm$ did couple strongly to the cyanobacteria and the splitting energy was reduced between the two modes during persistent irradiation (Fig. 5A, blue dashed line). Fig. 5B shows the first (blue line) and the last (red line) spectrum of the spectral series in Fig. 5A and obviously the splitting between the two modes is reduced. The temporal evolution for two different spatial positions is shown in Fig. 5C and regardless of the spatial position the spectral splitting is reduced. The number of molecules (*n* in Eq. 1) is reduced exponentially during irradiation, therefore the spectral splitting between the coupled modes does decrease with the square root of an exponential decay, which is shown by the solid lines in Fig. 5C. These results demonstrate that the splitting energy depends on the number of pigments participating in the coupling, and suggest that all fluorophores in the focus are coherently coupled to the cavity mode and consequently that the cavity induces a coherence of all pigments in the photosynthetic machinery at ambient conditions.

Conclusion

The results presented here demonstrate indubitably that an *in vivo* coherent, quantum optical energy exchange between the microcavity and the bacterial photosynthetic machinery exists. As the microcavity interferes with the coherence of the entire range of pigments in the photosynthetic complexes, which requires their defined spatial organization and compensation for thermodynamic fluctuations at ambient temperature, it is very likely that this quantum physical process is not merely a by-product of evolution. On the contrary, evolution has obviously selected for the quantum mechanical process of coherence to optimize photosynthesis to its highest efficiency. Accordingly, the model of a wave-like energy transfer should replace the classical model of energy hopping in the photosynthetic light-harvesting process (Fig. 1A/B). Our validation of coherent quantum mechanics in the photosynthetic machinery of living cyanobacteria, at physiologically relevant conditions, entails the re-evaluation of quantum mechanics in various other biological processes.

Acknowledgment

A.J.M., F.W. and K.H. acknowledge support by the VW foundation (project title: A quantum beat for life) and the Deutsche Forschungsgemeinschaft (ME 1600/13-3; HA 2146/23-1). The authors would like to thank F. de Courcy for English proofreading of the manuscript.

Literature

(1) Schrödinger, E. *What Is Life?*; Cambridge University Press, 1944.

(2) Davydov, A. S. (Aleksandr S., 1912-. *Biology & Quantum Mechanics / by A.S. Davydov ; Translated by D. Oliver*; International series in natural philosophy ; v. 109.; Pergamon Press: Oxford ; New York, 1982.

(3) Fleming, G. R.; Scholes, G. D.; Cheng, Y.-C. Quantum Effects in Biology. *Procedia Chem.* **2011**, *3* (1), 38–57. https://doi.org/10.1016/j.proche.2011.08.011.

(4) Panitchayangkoon, G.; Hayes, D.; Fransted, K. A.; Caram, J. R.; Harel, E.; Wen, J.; Blankenship, R. E.; Engel, G. S. Long-Lived Quantum Coherence in Photosynthetic Complexes at Physiological Temperature. *Proc. Natl. Acad. Sci.* **2010**, *107* (29), 12766–12770. https://doi.org/10.1073/pnas.1005484107.

(5) De Vault, D.; Chance, B. Studies of Photosynthesis Using a Pulsed Laser. *Biophys. J.* **1966**, *6* (6), 825–847. https://doi.org/10.1016/S0006-3495(66)86698-5.

(6) Marcus, R. A. H and Other Transfers in Enzymes and in Solution: Theory and Computations, a Unified View. 2. Applications to Experiment and Computations †. *J. Phys. Chem. B* **2007**, *111* (24), 6643–6654. https://doi.org/10.1021/jp071589s.

(7) Bandyopadhyay, J. N.; Paterek, T.; Kaszlikowski, D. Quantum Coherence and Sensitivity of Avian Magnetoreception. *Phys. Rev. Lett.* **2012**, *109* (11). https://doi.org/10.1103/PhysRevLett.109.110502.

(8) Scholes, G. D. Quantum-Coherent Electronic Energy Transfer: Did Nature Think of It First? *J. Phys. Chem. Lett.* **2010**, *1* (1), 2–8. https://doi.org/10.1021/jz900062f.

(9) Engel, G. S.; Calhoun, T. R.; Read, E. L.; Ahn, T.-K.; Mančal, T.; Cheng, Y.-C.; Blankenship, R. E.; Fleming, G. R. Evidence for Wavelike Energy Transfer through Quantum Coherence in Photosynthetic Systems. *Nature* **2007**, *446* (7137), 782–786. https://doi.org/10.1038/nature05678.

(10) Fassioli, F.; Dinshaw, R.; Arpin, P. C.; Scholes, G. D. Photosynthetic Light Harvesting: Excitons and Coherence. *J. R. Soc. Interface* **2014**, *11* (92), 20130901. https://doi.org/10.1098/rsif.2013.0901.

(11) Fassioli, F.; Olaya-Castro, A. Distribution of Entanglement in Light-Harvesting Complexes and Their Quantum Efficiency. *New J. Phys.* **2010**, *12* (8), 085006. https://doi.org/10.1088/1367-2630/12/8/085006.

(12) Karafyllidis, I. G. Quantum Transport in the FMO Photosynthetic Light-Harvesting Complex. *J. Biol. Phys.* **2017**, *43* (2), 239–245. https://doi.org/10.1007/s10867-017-9449-4.

(13) Collini, E.; Wong, C. Y.; Wilk, K. E.; Curmi, P. M. G.; Brumer, P.; Scholes, G. D. Coherently Wired Light-Harvesting in Photosynthetic Marine Algae at Ambient Temperature. *Nature* **2010**, *463* (7281), 644–647. https://doi.org/10.1038/nature08811.

(14) Cheng, Y.-C.; Fleming, G. R. Dynamics of Light Harvesting in Photosynthesis. *Annu. Rev. Phys. Chem.* **2009**, *60* (1), 241–262. https://doi.org/10.1146/annurev.physchem.040808.090259.

(15) Hildner, R.; Brinks, D.; Nieder, J. B.; Cogdell, R. J.; van Hulst, N. F. Quantum Coherent Energy Transfer over Varying Pathways in Single Light-Harvesting Complexes. *Science* **2013**, *340* (6139), 1448–1451. https://doi.org/10.1126/science.1235820.

(16) Ishizaki, A.; Fleming, G. R. Quantum Superpositions in Photosynthetic Light Harvesting: Delocalization and Entanglement. *New J. Phys.* **2010**, *12* (5), 055004. https://doi.org/10.1088/1367-2630/12/5/055004.

(17) Coles, D.; Flatten, L. C.; Sydney, T.; Hounslow, E.; Saikin, S. K.; Aspuru-Guzik, A.; Vedral, V.; Tang, J. K.-H.; Taylor, R. A.; Smith, J. M.; et al. A Nanophotonic Structure Containing Living Photosynthetic Bacteria. *Small* **2017**, *13* (38), 1701777. https://doi.org/10.1002/smll.201701777.

(18) Rexroth, S.; Nowaczyk, M. M.; Rögner, M. Cyanobacterial Photosynthesis: The Light Reactions. In *Modern Topics in the Phototrophic Prokaryotes: Metabolism, Bioenergetics, and Omics*; Hallenbeck, P. C., Ed.; Springer International Publishing: Cham, 2017; pp 163–191. https://doi.org/10.1007/978-3-319-51365-2_5.

(19) Watanabe, M.; Ikeuchi, M. Phycobilisome: Architecture of a Light-Harvesting Supercomplex. *Photosynth. Res.* **2013**, *116* (2–3), 265–276. https://doi.org/10.1007/s11120-013-9905-3.

(20) Stadnichuk, I. N.; Krasilnikov, P. M.; Zlenko, D. V. Cyanobacterial Phycobilisomes and Phycobiliproteins. *Microbiology* **2015**, *84* (2), 101–111. https://doi.org/10.1134/S0026261715020150.

(21) Groot, M. L.; Pawlowicz, N. P.; van Wilderen, L. J. G. W.; Breton, J.; van Stokkum, I. H. M.; van Grondelle, R. Initial Electron Donor and Acceptor in Isolated Photosystem II Reaction Centers Identified with Femtosecond Mid-IR Spectroscopy. *Proc. Natl. Acad. Sci.* **2005**, *102* (37), 13087–13092. https://doi.org/10.1073/pnas.0503483102.

(22) Holzwarth, A. R.; Muller, M. G.; Reus, M.; Nowaczyk, M.; Sander, J.; Rogner, M. Kinetics and Mechanism of Electron Transfer in Intact Photosystem II and in the Isolated Reaction Center: Pheophytin Is the Primary Electron Acceptor. *Proc. Natl. Acad. Sci.* **2006**, *103* (18), 6895–6900.

https://doi.org/10.1073/pnas.0505371103.
(23) Adir, N.; Bar-Zvi, S.; Harris, D. The Amazing Phycobilisome. *Biochim. Biophys. Acta BBA - Bioenerg.* **2019**. https://doi.org/10.1016/j.bbabio.2019.07.002.
(24) van Grondelle, R.; Dekker, J. P.; Gillbro, T.; Sundstrom, V. Energy Transfer and Trapping in Photosynthesis. *Biochim. Biophys. Acta BBA - Bioenerg.* **1994**, *1187* (1), 1–65. https://doi.org/10.1016/0005-2728(94)90166-X.
(25) Doerrich, A.; Wilde, A. Spot Assays for Viability Analysis of Cyanobacteria. *BIO-Protoc.* **2015**, *5* (17). https://doi.org/10.21769/BioProtoc.1574.
(26) Konrad, A.; Metzger, M.; Kern, A. M.; Brecht, M.; Meixner, A. J. Controlling the Dynamics of Förster Resonance Energy Transfer inside a Tunable Sub-Wavelength Fabry–Pérot-Resonator. *Nanoscale* **2015**, *7* (22), 10204–10209. https://doi.org/10.1039/C5NR02027A.
(27) Rippka, R.; Stanier, R. Y.; Deruelles, J.; Herdman, M.; Waterbury, J. B. Generic Assignments, Strain Histories and Properties of Pure Cultures of Cyanobacteria. *Microbiology* **1979**, *111* (1), 1–61. https://doi.org/10.1099/00221287-111-1-1.
(28) Watzer, B.; Spät, P.; Neumann, N.; Koch, M.; Sobotka, R.; Macek, B.; Hennrich, O.; Forchhammer, K. The Signal Transduction Protein PII Controls Ammonium, Nitrate and Urea Uptake in Cyanobacteria. *Front. Microbiol.* **2019**, *10*. https://doi.org/10.3389/fmicb.2019.01428.
(29) Kondou, Y.; Nakazawa, M.; Higashi, S.; Watanabe, M.; Manabe, K. Equal-Quantum Action Spectra Indicate Fluence-Rate-Selective Action of Multiple Photoreceptors for Photomovement of the Thermophilic Cyanobacterium Synechococcus Elongatus¶. *Photochem. Photobiol.* **2007**, *73* (1), 90–95. https://doi.org/10.1562/0031-8655(2001)0730090EQASIF2.0.CO2.
(30) Kennis, J. T. M.; Gobets, B.; van Stokkum, I. H. M.; Dekker, J. P.; van Grondelle, R.; Fleming, G. R. Light Harvesting by Chlorophylls and Carotenoids in the Photosystem I Core Complex of *Synechococcus Elongatus* : A Fluorescence Upconversion Study. *J. Phys. Chem. B* **2001**, *105* (19), 4485–4494. https://doi.org/10.1021/jp010382a.
(31) Lahmi, R.; Sendersky, E.; Perelman, A.; Hagemann, M.; Forchhammer, K.; Schwarz, R. Alanine Dehydrogenase Activity Is Required for Adequate Progression of Phycobilisome Degradation during Nitrogen Starvation in Synechococcus Elongatus PCC 7942. *J. Bacteriol.* **2006**, *188* (14), 5258–5265. https://doi.org/10.1128/JB.00209-06.
(32) Damjanović, A.; Vaswani, H. M.; Fromme, P.; Fleming, G. R. Chlorophyll Excitations in Photosystem I of *Synechococcus Elongatus*. *J. Phys. Chem. B* **2002**, *106* (39), 10251–10262. https://doi.org/10.1021/jp020963f.
(33) Lakowicz, J. R. *Principles of Fluorescence Spectroscopy*, 3rd ed.; Springer: New York, 2006.
(34) Byrdin, M.; Rimke, I.; Schlodder, E.; Stehlik, D.; Roelofs, T. A. Decay Kinetics and Quantum Yields of Fluorescence in Photosystem I from Synechococcus Elongatus with P700 in the Reduced and Oxidized State: Are the Kinetics of Excited State Decay Trap-Limited or Transfer-Limited? *Biophys. J.* **2000**, *79* (2), 992–1007. https://doi.org/10.1016/S0006-3495(00)76353-3.
(35) Fišerová, E.; Kubala, M. Mean Fluorescence Lifetime and Its Error. *J. Lumin.* **2012**, *132* (8), 2059–2064. https://doi.org/10.1016/j.jlumin.2012.03.038.
(36) Purcell, E. M. Spontaneous Emission Probabilities at Radio Frequencies. In *Confined Electrons and Photons: New Physics and Applications*; Burstein, E., Weisbuch, C., Eds.; Springer US: Boston, MA, 1995; pp 839–839. https://doi.org/10.1007/978-1-4615-1963-8_40.
(37) Fox, M. *Quantum Optics: An Introduction*; Oxford master series in physics; Oxford University Press: Oxford ; New York, 2006.
(38) Junginger, A.; Wackenhut, F.; Stuhl, A.; Blendinger, F.; Brecht, M.; Meixner, A. J. Tunable Strong Coupling of Two Adjacent Optical λ/2 Fabry-Pérot Microresonators. *ArXiv E-Prints* **2019**, arXiv:1908.01566.
(39) Marletto, C.; Coles, D. M.; Farrow, T.; Vedral, V. Entanglement between Living Bacteria and Quantized Light Witnessed by Rabi Splitting. *J. Phys. Commun.* **2018**, *2* (10), 101001. https://doi.org/10.1088/2399-6528/aae224.